

# Performance of a Cooperative Network using Rate Adaptation and Cooperative Combining

Prasanna Kalansuriya, Madushanka Soysa and Chinthia Tellambura  
 Department of Electrical and Computer Engineering  
 University of Alberta, Edmonton, Alberta, Canada T6G 2V4  
 Email: {kalansur, soysa, chinthia}@ece.ualberta.ca

**Abstract**—The performance of a cooperative network with Cooperative Maximal Ratio Combining (C-MRC) is analyzed. To this end, we propose a heuristic approximation to the total received SNR (signal-to-noise ratio) at the destination. The approximation is not only an accurate representation of the received SNR, but also amenable to performance analysis. We then derive the probability density function (PDF) of the approximate SNR. The PDF is used to derive expressions of the parameters required for the performance analysis of rate adaptive transmission, based on the use of a discrete set of modes of square  $M$ -ary quadrature amplitude modulation (QAM), with a cooperative network employing C-MRC. Analytical expressions for mode selection probability, the outage probability, the average spectral efficiency, and the average bit error rate are derived. Results show that performance of the system under C-MRC is comparable with other cooperative networks.

**Index Terms**—Adaptive transmission, Decode-and-forward, Cooperative MRC, Nakagami- $m$  fading.

## I. INTRODUCTION

Consumer demand for low-cost, high-speed, high-quality mobile content delivery has fueled a phenomenal growth in the wireless communication industry during the past few decades. As a result new wireless technologies and standards have emerged to satisfy the ever increasing demand for mobile and wireless connectivity. Current research aims at improving the capabilities of wireless communication in beyond third generation (B3G), fourth generation wireless 4G technologies and beyond.

Cooperative wireless communication [1], [2] is an active research area where the cooperation of a network of single-antenna wireless devices creates a virtual multiple antenna system and provides diversity in terms of spatial separation. Adaptive transmission [3]–[6] is another technique used to enhance the throughput of wireless channels under the impairments of multipath fading and shadowing. The transmitter uses channel state information (CSI) to take advantage of the variations of the wireless channel. A series of recent papers [7]–[12] have investigated the use of adaptive strategies with cooperative networks. In [7] the limits of achievable capacity of a cooperative network under different adaptive transmission techniques was investigated. Nechiporenko et. al. extended the work of [7] to a multiple amplify-and-forward (AF) relay cooperative network in [9]. The practical technique of adaptive discrete rate  $M$ -QAM was considered for cooperative networks in [10]–[12]. In all the aforementioned work under

adaptive transmission in conjunction with cooperative diversity, the analysis for decode-and-forward (DF) cooperative networks is performed under the assumption of error-free decoding at relays.

Relaying is pivotal to the operation of a cooperative wireless system. We focus our attention on regenerative (decode-and-forward) relays. Such relays decode and retransmit the received signal to the destination. However, error propagation can occur due to decoding errors. Hence, cooperative demodulation techniques are required at the destination where signals are combined to benefit from the cooperative diversity provided by the network. Several techniques for cooperative demodulation and detection have been proposed in the literature. Reference [13] presents a maximum likelihood (ML) optimal detector for BPSK (binary phase shift keying). Due to the complexity of performance analysis using the optimal detector, [13] also provides a suboptimal combiner termed  $\lambda$ -MRC. A piece-wise linear (PL) near-ML decoder is derived for coherent and non-coherent BFSK in [14]. Reference [15] provides a low-complexity method termed Cooperative Maximal Ratio Combining (C-MRC), which tightly lower bounds the performance of ML detection. Reference [16] presents the product MRC (P-MRC) scheme, which requires significantly low signaling overhead than C-MRC. Most of these techniques require the destination to have knowledge of the instantaneous CSI or bit error rate (BER) at the relays.

In this paper we investigate the performance of a cooperative network using C-MRC with rate adaptive transmission. We consider a regenerative cooperative network consisting of  $N$  parallel cooperative relays. A novel heuristic approximation for the total received signal-to-noise ratio (SNR) is developed. The probability density function (PDF) of the approximate SNR is derived and is used for the subsequent performance analysis. Adaptive transmission is based on a discrete mode adaptive scheme [17], which uses transmission modes consisting of square  $M$ -ary quadrature amplitude modulation ( $M$ -QAM) constellations. The mode selection probability, the outage probability, the average spectral efficiency, and the average bit error rate are derived. Results show that performance of the system under C-MRC is comparable with other cooperative networks.

## II. SYSTEM AND CHANNEL MODEL

The regenerative or decode-and-forward (DF) cooperative network is illustrated in Fig. 1. In this model the transmission

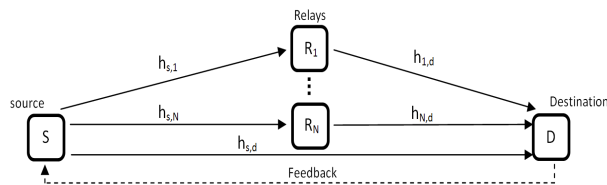


Fig. 1. System model.

of the source ( $S$ ) is assisted by  $N \geq 1$  number of cooperative relays. The cooperative protocol involves two phases. During the first phase, the source transmits its message  $x$  which is received by the destination and all the  $N$  relays due to the broadcast nature of the wireless channel. The received message at the destination and the  $i$ th ( $i = 1, \dots, N$ ) relay are  $r_{s,d} = h_{s,d}\sqrt{E_s}x + n_{s,d}$  and  $r_{s,i} = h_{s,i}\sqrt{E_s}x + n_{s,i}$  where  $x$  is the transmit symbol and  $E_s$  is the average transmit power. In the second phase, each of the relays transmits the message received from the source through an orthogonal channel to the destination which are then combined using the C-MRC technique. The received signal at the destination from the  $i$ th relay during the second phase is  $r_{i,d} = h_{i,d}\sqrt{E_s}\hat{x} + n_{i,d}$  where  $\hat{x}$  is the decoded and re-encoded symbol of  $x$ .  $n_{s,i}$ ,  $n_{s,d}$  and  $n_{i,d}$  are the noise present at the relays and the destination. All noise samples are modeled as additive white Gaussian noise (AWGN). The wireless environment is modeled using the Nakagami- $m$  fading distribution. For simplicity, we assume all channel gains between wireless nodes to be independent and identically distributed (i.i.d.). Although our results can be extended to the non-i.i.d. case, it is omitted for brevity.

### III. RATE ADAPTIVE TRANSMISSION

Rate adaptive transmission is implemented using a discrete set of transmission modes. The transmission mode is changed based on a channel quality measurement done at the destination. Under this adaptive scheme source transmission takes places with a constant average power, and the transmission data rate will vary according to the channel conditions. Furthermore, the adaptation improves the overall spectral efficiency while maintaining a quality of service (QoS) constraint, say, in terms of a target BER.

The range of received SNR is partitioned into  $K$  regions using a set of switching levels  $\mathbf{S} = \{\gamma_n | n = 0, 1, \dots, K\}$  with  $K = 5$  being considered for our analysis which was termed **five-mode AQAM** [17]. The transmitter selects mode  $n$  when the received SNR falls in the  $n$ th region; i.e.  $\gamma_n \leq \gamma_{tot} < \gamma_{n+1}$ . Information of which transmission mode to be used, i.e.,  $n$ , is communicated to the source through reliable, low delay feedback link (Fig. 1). It is assumed that this feedback link is error free. When the transmitter switches between different modes, the relays need to identify the correct mode being transmitted. For this purpose, the transmitter may have to send side information to the relays, or potentially the relays may employ automatic modulation classification techniques [18], [19] to identify the incoming modulation mode without side information.

Table I summarizes the parameters of the five-mode AQAM scheme, where  $b_n$  is the number of bits per transmitted symbol,  $\gamma$  is the instantaneous received SNR and  $M_n$  is the constellation size of the modulation scheme of the  $n$ th mode. BPSK, QPSK, 16-QAM, 64-QAM have been considered in four of the five modes since they are widely used in many existing standards [20], [21] and since they have been extensively studied under adaptive modulation in literature [5], [17].

In our analysis we consider the switching level assignment proposed in [6]. Under this method each switching level is chosen so that the two modes being separated by the switching level would satisfy a BER constraint under AWGN conditions at the SNR value of switching. Particularly, the higher of the two modes should yield a BER approximately equal to the BER target. The switching levels would be determined as follows

$$\begin{aligned} \gamma_0 &= 0 \\ \gamma_1 &= [\text{erfc}^{-1}(2\text{BER}_0)]^2, \\ \gamma_n &= \frac{2}{3}K_0(M_n - 1); \quad n = 2, 3, \dots, K - 1, \\ \gamma_K &= +\infty, \end{aligned} \quad (1)$$

where  $\text{BER}_0$  is the target BER level,  $\text{erfc}^{-1}(\cdot)$  is the inverse complementary error function and  $K_0 = -\ln(5\text{BER}_0)$ .

### IV. SNR APPROXIMATION FOR C-MRC

We have chosen C-MRC proposed in [15], [22] for the cooperative demodulation of received signals at the destination because of its low complexity and near-ML performance. Furthermore, the implementation of ML detection for higher order constellations, considered in our adaptive scheme, becomes exceedingly complicated with the presence of errors at the relays.

According to [15] the combining of received signals  $r_{s,d}$  and  $r_{i,d}$ ,  $i \in \{1, \dots, N\}$  using C-MRC is done as follows

$$r = w_{s,d}r_{s,d} + \sum_{i=1}^N w_{i,d}r_{i,d}, \quad (2)$$

where  $w_{s,d}$  and  $w_{i,d}$  are weights which are functions of  $h_{s,d}$ ,  $h_{s,i}$  and  $h_{i,d}$ . The weight  $w_{s,d}$  is chosen to be  $w_{s,d} = h_{s,d}^*$  as in the case of MRC. However, for determining the weight  $w_{i,d}$ , which has to account for the errors introduced at the relay, the end-to-end equivalent SNR for the path via the  $i$ th relay is required. Hence,  $w_{i,d}$  is chosen as

$$w_{i,d} = \frac{\gamma_{eq}}{\gamma_{i,d}} h_{i,d}^*, \quad (3)$$

where  $\gamma_{eq}$  is the equivalent one-hop received SNR for the two hop path via the  $i$ th relay. It was shown in [15], [22] that  $\gamma_{eq}$  is bounded as  $\gamma_{min} - \frac{3.24}{\alpha} < \gamma_{eq} \leq \gamma_{min}$  where  $\gamma_{min} = \min(\gamma_{s,i}, \gamma_{i,d})$ . Therefore, we have approximated  $\gamma_{eq}$  as  $\gamma_{eq} \approx \min(\gamma_{s,i}, \gamma_{i,d})$ . Under this approximation when  $\gamma_{s,i} > \gamma_{i,d}$ ,  $w_{i,d}$  reverts to conventional MRC which makes  $w_{i,d} = h_{i,d}^*$ , i.e. the combiner is more confident that the symbols arriving from the relay are accurate since the source to relay link has better quality than the relay to destination link. When  $\gamma_{s,i} < \gamma_{i,d}$  the combiner has low confidence on the reliability of the symbol arriving at the relay.

The detected symbol at the destination  $\tilde{x}$  is given as

$$\tilde{x} = \arg \min_{x \in A_x} \left| w_{s,d} r_{s,d} + \sum_{i=1}^N w_{i,d} r_{i,d} - \left( w_{s,d} h_{s,d} + \sum_{i=1}^N w_{i,d} h_{i,d} \right) x \right|^2, \quad (4)$$

where  $A_x$  is the set of constellation points or symbols of the constellation considered for transmission. The analysis carried out in [15], [22] proves that C-MRC provides full diversity benefits at the destination. However, they do not provide a closed form solution for the total received SNR at the destination.

To use C-MRC in the adaptive scheme described in Section III, an expression for the instantaneous total received SNR at the destination is required. The derivation of an analytical closed form expression for the total received SNR appears to be complicated with C-MRC. Also, such an expression may also be dependent on the mode being used for transmission (since bit errors caused at the relays depend on the modulation scheme employed). Due to these difficulties of deriving an exact expression for the total received SNR for C-MRC, we have resorted to the use of an approximation for the received SNR, which is independent of the underlying modulation scheme used. We have tried several heuristic approximations for the total received SNR which were tested through Monte Carlo simulations using a trial and error approach. Simulations were performed extensively under Rayleigh, Ricean and Nakagami- $m$  fading models and in i.i.d. and non-i.i.d. fading environments with different numbers of cooperating DF relays. The decoding at the relays was carried out using ML detection and received signals were combined at the destination using C-MRC according to (2) and symbol detection was performed using (4). The Nakagami- $m$  random variables required for simulating the faded envelop was generated using the method proposed in [23]. From our numerical experiments, we find that (5) is an accurate representation of the total received SNR at the destination:

$$\gamma_{ap} = \gamma_{s,d} + \sum_{i=1}^N 0.5 \min(\gamma_{s,i}, \gamma_{i,d}). \quad (5)$$

The accuracy of (5) is shown in Fig. 2, where the BER curves are obtained for a cooperative network (non-adaptive constant rate) consisting of two DF relays under i.i.d. Nakagami- $m$  fading with  $m = 2$  for four different modulation schemes. From the BER curves we observe that  $\gamma_{ap}$  provides a very accurate approximation to the total received SNR at the destination under C-MRC.

Fig. 3 depicts the outage probability associated with a two DF relay cooperative network and 4-QAM. Outage probability for C-MRC was derived using BER simulation results considering a BER based outage threshold of 0.01. A BER above this threshold was considered to result in an outage event. The corresponding theoretical C-MRC plot for outage probability was derived by using the approximation for received SNR  $\gamma_{ap}$  and considering a equivalent outage SNR threshold of 7.33 dB (for 4-QAM, this threshold of 7.33 dB results in a

TABLE I  
FIVE-MODE ADAPTIVE  $M$ -QAM PARAMETERS

SNR	$n$	$M_n$	$b_n$	mode
$\gamma_0 \leq \gamma < \gamma_1$	0	0	0	No Tx
$\gamma_1 \leq \gamma < \gamma_2$	1	2	1	BPSK
$\gamma_2 \leq \gamma < \gamma_3$	2	4	2	QPSK
$\gamma_3 \leq \gamma < \gamma_4$	3	16	4	16-QAM
$\gamma_4 \leq \gamma < \gamma_5$	4	64	6	64-QAM

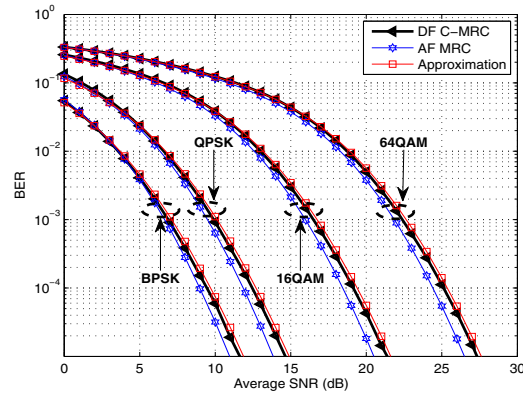


Fig. 2. BER of a 2 relay network for  $M$ -QAM ( $M = 2, 4, 16, 64$ ) with Nakagami- $m$  fading ( $m = 2$ ).

BER of 0.01). From the plots it is clear that  $\gamma_{ap}$  serves as a good approximation for the received SNR in terms of outage probability.

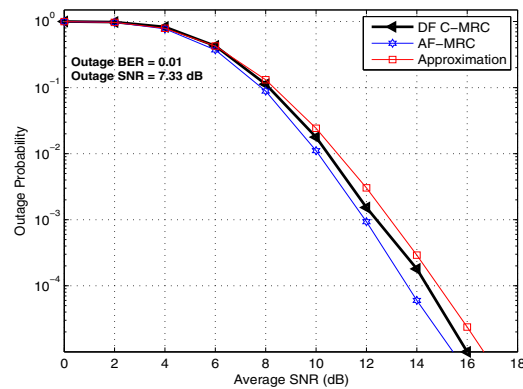


Fig. 3. Outage probability for 4-QAM, with i.i.d. Nakagami- $m$  fading,  $m = 2$ , two relay network.

## V. PERFORMANCE PARAMETERS FOR RATE ADAPTIVE TRANSMISSION

The analysis of C-MRC under five-mode AQAM is performed by using the proposed approximation for the received SNR at the destination given by  $\gamma_{ap}$  in (6). Therefore, the total received SNR at the destination is

$$\gamma_{tot} \approx \gamma_{s,d} + \sum_{i=1}^N 0.5 \min(\gamma_{s,i}, \gamma_{i,d}). \quad (6)$$

$$\delta_n = \frac{\Gamma^N(2m)}{2^{2N(m-1)} m^N \Gamma^{2N}(m)} \left\{ \sum_{r=1}^m \frac{\Lambda_r}{\Gamma(r)} \left[ \Gamma\left(r, \frac{m\gamma_n}{\bar{\gamma}}\right) - \Gamma\left(r, \frac{m\gamma_{n+1}}{\bar{\gamma}}\right) \right] + \sum_{t=1}^{N(2m-1)} \frac{\Omega_t}{\Gamma(t)} \left[ \Gamma\left(t, \frac{4m\gamma_n}{\bar{\gamma}}\right) - \Gamma\left(t, \frac{4m\gamma_{n+1}}{\bar{\gamma}}\right) \right] \right\}. \quad (8)$$

$$\frac{R}{B} = \frac{\Gamma^N(2m)}{2^{2N(m-1)} m^N \Gamma^{2N}(m)(N+1)} \sum_{n=1}^{K-1} b_n \left\{ \sum_{r=1}^m \Lambda_r \left[ \frac{\Gamma\left(r, \frac{m\gamma_n}{\bar{\gamma}}\right) - \Gamma\left(r, \frac{m\gamma_{n+1}}{\bar{\gamma}}\right)}{\Gamma(r)} \right] + \sum_{t=1}^{N(2m-1)} \Omega_t \left[ \frac{\Gamma\left(t, \frac{4m\gamma_n}{\bar{\gamma}}\right) - \Gamma\left(t, \frac{4m\gamma_{n+1}}{\bar{\gamma}}\right)}{\Gamma(t)} \right] \right\}. \quad (9)$$

$$P_n = \frac{\Gamma^N(2m)}{2^{2N(m-1)} m^N \Gamma^{2N}(m)} \left[ \sum_{r=1}^m \frac{\Lambda_r}{(r-1)!} \left(\frac{m}{\bar{\gamma}}\right)^r \sum_l A_l I_r(a_l, m/\bar{\gamma}, \gamma_n, \gamma_{n+1}) + \sum_{t=1}^{N(2m-1)} \frac{\Omega_t}{(t-1)!} \left(\frac{4m}{\bar{\gamma}}\right)^t \sum_l A_l I_t(a_l, 4m/\bar{\gamma}, \gamma_n, \gamma_{n+1}) \right]. \quad (10)$$

The PDF of approximation for  $\gamma_{\text{tot}}$  is derived in Appendix A. Using this PDF (23) mathematical expressions are derived for the performance parameters considered in our analysis.

1) **Mode Selection Probability:** This is the probability that the received SNR would fall in the  $n$ th partition, resulting the use of the  $n$ th mode by the transmitter. By using the PDF (23) in [17, Eq. (2)] the MSP is derived to be (8) where  $\Lambda_r$  and  $\Omega_t$  are given in (21) and (22) respectively.

2) **Outage Probability:** When the SNR falls below the first switching level of  $\gamma_1$ , the transmitter selects the no-transmit mode. The outage event caused by this can be found as

$$P_{\text{out}} = 1 - \frac{\Gamma^N(2m)}{2^{2N(m-1)} m^N \Gamma^{2N}(m)} \left\{ \sum_{r=1}^m \Lambda_r \frac{\Gamma\left(r, \frac{m\gamma_1}{\bar{\gamma}}\right)}{\Gamma(r)} + \sum_{t=1}^{N(2m-1)} \Omega_t \frac{\Gamma\left(t, \frac{4m\gamma_1}{\bar{\gamma}}\right)}{\Gamma(t)} \right\}. \quad (10)$$

3) **Average Spectral Efficiency:** The average spectral efficiency can be derived by using the MSP  $\delta_n$  in [6, Eq. (33)]. It is derived to be (9), note that the division by  $N+1$  is required since  $N+1$  orthogonal channels are used in the transmission of information from source to destination.

4) **Average Bit Error Rate:** Since different modulation schemes are being employed under varying channel conditions with signal fading (Table I), an average BER value is needed which averages the effects of both fading and the use of different modulation schemes. The average BER for five-mode AQAM scheme is given as [17]

$$BER_{\text{avg}} = \frac{\sum_{n=1}^{K-1} b_n P_n}{\sum_{n=1}^{K-1} b_n \delta_n}, \quad (11)$$

where  $P_n$  is the BER of the  $n$ th transmission mode which is calculated as

$$P_n = \int_{\gamma_n}^{\gamma_{n+1}} P_{M_n, \text{QAM}}(\gamma) f_{\gamma_{\text{tot}}}(\gamma) d\gamma. \quad (12)$$

$P_{M_n, \text{QAM}}$  is the BER of square M-QAM in an AWGN channel, with coherent detection and Gray coding given as [17]

$$P_{M_n, \text{QAM}} = \sum_l A_l Q(\sqrt{a_l \bar{\gamma}}), \quad (13)$$

where  $Q(\cdot)$  is the standard Gaussian Q-function defined as  $Q(x) = \frac{1}{\sqrt{2\pi}} \int_x^\infty e^{-z^2/2} dz$ ,  $\gamma$  is the received SNR, and  $A_l$  and  $a_l$  are constants particular to the QAM constellation used, given in [17]. Using (23), (12) and (13) expression for  $P_n$  is derived to be (10) where  $I_i(a_l, \beta, \gamma_n, \gamma_{n+1})$  is evaluated in closed form in [11].

## VI. SIMULATION RESULTS

The results from analytical equations derived from the approximation to received SNR  $\gamma_{\text{ap}}$  and the simulation results are compared. Simulations were performed on a system consisting of 2 DF cooperative relays where all channels are modeled as i.i.d. Nakagami- $m$  with  $m=2$ . Simulation results were also obtained for a comparable AF cooperative network and an adaptive DF cooperative network discussed in our previous work of [11] and [12].

The average spectral efficiency is depicted in Fig. 4. Both C-MRC method and the AF system with MRC method perform equally well while the adaptive DF system performs the best, achieving gains ranging from 2.5 dB to 3 dB for a given average spectral efficiency. The simulation results and theoretical values of the C-MRC system agree well.

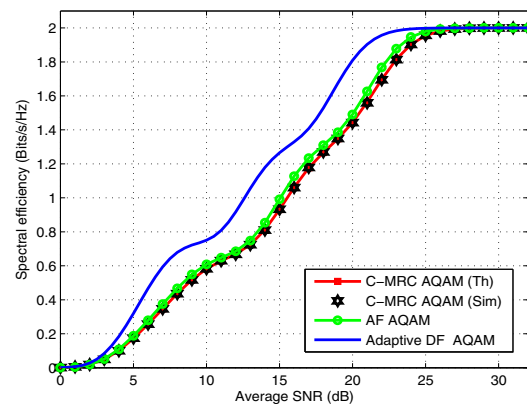


Fig. 4. Average spectral efficiency, with i.i.d. Nakagami- $m$  fading,  $m=2$ , two relay network.

The average BER curves of C-MRC are shown in Fig. 5. Except initially, the BER curves stay below the target BER

constraint of  $10^{-3}$ . The theoretical curve gives a lower average BER than the simulation results. Furthermore, it is observed that the gap between the theoretical BER approximation and the simulation result has increased for rate adaptive transmission, unlike that of the fixed rate transmission (Fig. 2). However, it should be noted that for non-adaptive fixed rate transmission the average BER is obtained by averaging over all possible channel conditions for a particular fixed modulation scheme. But in the rate adaptive scheme simulated here, the instantaneous BER of higher modulation schemes depend on favorable channel conditions while the instantaneous BER of lower modulation schemes relate to poor channel conditions, due to the switching levels employed. Hence, the accuracy of the approximation for total received SNR under C-MRC is reduced when rate adaptive transmission is considered. This conclusion is further supported from the observation that for higher SNR values, say above 25 dB, the simulation and theoretical curves overlap and show a good match, where the transmitter selects the highest mode with a very high probability (very low probability of switching to lower modes at high average SNR values). At the high SNR region since the transmitter operation is similar to a non-adaptive fixed rate transmitter the simulation and theoretical results are in accordance as opposed to lower SNR regions where adaptation is employed. The average BER curve obtained with 64-QAM using C-MRC is also given in the figure. For high SNR values, all curves show the same diversity order.

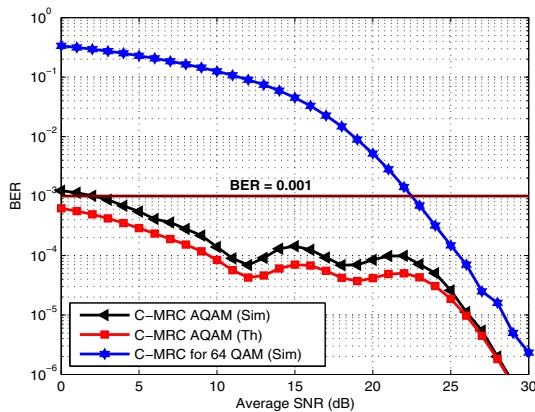


Fig. 5. Average BER for system using C-MRC, with i.i.d. Nakagami- $m$  fading,  $m = 2$ , two relay network.

## VII. CONCLUSION

A heuristic approximation for received SNR of a relay system with C-MRC was proposed. The approximation is justified via extensive simulations. The PDF of the received SNR for an i.i.d. Nakagami- $m$  fading environment was derived. Decoding errors at relays are accounted into the final result observed at the destination receiver through the use of cooperative demodulation and symbol detection. Results show that the rate adaptive system with C-MRC maintains desired QoS constraint while exploiting the channel variation to improve average throughput. The performance of other cooperative

systems was compared with that of the C-MRC system. When compared to the Adaptive DF system proposed in [12] where error-free decoding was assumed (with a decoding SNR threshold) the system under C-MRC shows a 2.5 dB to 3 dB gain loss for a given average spectral efficiency due to the presence of decoding errors at relays.

## APPENDIX

It is shown in [24] for i.i.d. Nakagami- $m$  fading the moment generating function (MGF) of  $\gamma_i = \min(\gamma_{s,i}, \gamma_{i,d})$  can be written as

$$M_{\gamma_i}(s) = \left(\frac{m}{\bar{\gamma}}\right)^{2m} \frac{\Gamma(2m)}{m\Gamma^2(m)} \frac{2}{(2m/\bar{\gamma}+s)^{2m}} \times {}_2F_1\left(1, 2m; m+1; \frac{m/\bar{\gamma}+s}{2m/\bar{\gamma}+s}\right), \quad (14)$$

where  ${}_2F_1(\alpha, \beta; \gamma; z)$  is the hypergeometric function defined in [25, 9.100].

Using the transform of [25, 9.131]

$${}_2F_1\left(1, 2m; m+1; \frac{m/\bar{\gamma}+s}{2m/\bar{\gamma}+s}\right) = \frac{2m/\bar{\gamma}+s}{m/\bar{\gamma}} {}_2F_1\left(1, 1-m; m+1; -\frac{m/\bar{\gamma}+s}{m/\bar{\gamma}}\right) \quad (15)$$

and using the properties of [25, 9.100] for  $\beta < 0$  the hypergeometric series can be written as

$${}_2F_1\left(1, 1-m; m+1; -\frac{m/\bar{\gamma}+s}{m/\bar{\gamma}}\right) = \sum_{k=0}^{m-1} a_k \left(-\frac{m/\bar{\gamma}+s}{m/\bar{\gamma}}\right)^k \quad (16)$$

where  $a_k$  are the hypergeometric coefficients given by

$$a_0 = 1 \\ a_k = \frac{(1-m)(2-m)\dots(k-m)}{(m+1)(m+2)\dots(m+k)} \quad (17)$$

Substituting (16) into (15) then into (14) the MGF can be written as

$$M_{\gamma_i}(s) = \left(\frac{m}{\bar{\gamma}}\right)^{2m} \frac{\Gamma(2m)}{m\Gamma^2(m)} \frac{2}{(2m/\bar{\gamma}+s)^{2m}} \times \frac{2m/\bar{\gamma}+s}{m/\bar{\gamma}} \sum_{k=0}^{m-1} a_k \left(-\frac{m/\bar{\gamma}+s}{m/\bar{\gamma}}\right)^k \quad (18)$$

Replacing  $s$  by  $0.5s$  in (18) the MGF of  $0.5 \min(\gamma_{s,i}, \gamma_{i,d})$  can be derived. Therefore, the MGF of the total received SNR given in (6) can be written as,

$$M_{\gamma_{\text{tot}}}(s) = M_{\gamma_{s,d}}(s) \prod_{i=1}^N M_{\gamma_i}(0.5s) \quad (19)$$

Since  $\gamma_{s,d}$  is Gamma distributed with shape parameter  $m$  and scale parameter  $\bar{\gamma}/m$ ,  $M_{\gamma_{s,d}}(s)$  can be written as  $M_{\gamma_{s,d}}(s) = (1 + \bar{\gamma}/ms)^{-m}$ . Therefore, by using (18) with (19) we get

$$M_{\gamma_{\text{tot}}}(s) = \left[1 + \frac{\bar{\gamma}}{m}s\right]^{-m} \left[ \left(\frac{m}{\bar{\gamma}}\right)^{2m-1} \frac{\Gamma(2m)}{m\Gamma^2(m)} \frac{2}{(2m/\bar{\gamma} + 0.5s)^{2m-1}} \times \sum_{k=0}^{m-1} a_k \left(-\frac{m/\bar{\gamma} + 0.5s}{m/\bar{\gamma}}\right)^k \right]^N \quad (20)$$

$$\Lambda_r = \frac{\left(\frac{\bar{\gamma}}{m}\right)^{(r-m)}}{(m-r)!} \frac{\partial^{m-r}}{\partial s^{m-r}} \left[ \sum_{j=0}^{N(m-1)} \lambda_j \left(\frac{\bar{\gamma}}{2m} s\right)^j \left(1 + \frac{\bar{\gamma}}{4m} s\right)^{-N(2m-1)} \right]_{s=-m/\bar{\gamma}} \quad (21)$$

$$\Omega_t = \frac{\left(\frac{\bar{\gamma}}{4m}\right)^{(t-N(2m-1))}}{(N(2m-1)-t)!} \frac{\partial^{N(2m-1)-t}}{\partial s^{N(2m-1)-t}} \left[ \sum_{j=0}^{N(m-1)} \lambda_j \left(\frac{\bar{\gamma}}{2m} s\right)^j \left(1 + \frac{\bar{\gamma}}{m} s\right)^{-m} \right]_{s=-4m/\bar{\gamma}} \quad (22)$$

$$f_{\gamma_{\text{tot}}}(\gamma) = \frac{\Gamma^N(2m)}{2^{2N(m-1)} m^N \Gamma^{2N}(m)} \left[ \sum_{r=1}^m \frac{\Lambda_r}{(r-1)!} \left(\frac{m}{\bar{\gamma}}\right)^r \gamma^{r-1} e^{-\frac{\gamma m}{\bar{\gamma}}} + \sum_{t=1}^{N(2m-1)} \frac{\Omega_t}{(t-1)!} \left(\frac{4m}{\bar{\gamma}}\right)^t \gamma^{t-1} e^{-\frac{\gamma 4m}{\bar{\gamma}}} \right]. \quad (23)$$

By performing further simplifications we arrive at

$$M_{\gamma_{\text{tot}}}(s) = (0.5)^{2N(m-1)} \frac{\Gamma^N(2m)}{m^N \Gamma^{2N}(m)} \times \frac{\sum_{j=0}^{N(m-1)} \lambda_j \left(\frac{\bar{\gamma}}{2m} s\right)^j}{\left[1 + \frac{\bar{\gamma}}{m} s\right]^m \left[1 + \frac{\bar{\gamma}}{4m} s\right]^{N(2m-1)}}, \quad (24)$$

where  $\lambda_j = \frac{1}{j\delta_0} \sum_{r=1}^j (rN-j+r)\delta_r \lambda_{j-r}$  with  $\lambda_0 = \delta_0^N$  with  $j = 0, 1, \dots, N(m-1)$ .  $\delta_r$  are defined as  $\delta_r = \sum_{i=r}^{m-1} a_i (-1)^i \binom{i}{r}$  with  $r = 0, 1, \dots, m-1$ . Using partial fractions, (24) can be rewritten as

$$M_{\gamma_{\text{tot}}}(s) = (0.5)^{2N(m-1)} \frac{\Gamma^N(2m)}{m^N \Gamma^{2N}(m)} \left[ \sum_{r=1}^m \Lambda_r \left(1 + \frac{\bar{\gamma}}{m} s\right)^{-r} + \sum_{t=1}^{N(2m-1)} \Omega_t \left(1 + \frac{\bar{\gamma}}{4m} s\right)^{-t} \right], \quad (25)$$

where  $\Lambda_r$  and  $\Omega_t$  are given in (21) and (22) respectively. By taking the inverse Laplace transform of  $M_{\gamma_{\text{tot}}}(s)$  in (25), and using the fact that  $\mathcal{L}^{-1}\{(1+as)^{-k}\} = \frac{1}{(k-1)! a^k} x^{k-1} e^{-\frac{x}{a}}$ , the PDF of  $\gamma_{\text{tot}}$  is derived to be (23).

## REFERENCES

- [1] A. Sendonaris, E. Erkip, and B. Aazhang, "User cooperation diversity part I: system description," vol. 51, pp. 1927–1938, Nov. 2003.
- [2] J. N. Laneman, D. N. C. Tse, and G. W. Wornell, "Cooperative diversity in wireless networks: Efficient protocols and outage behavior," vol. 50, pp. 3062–3080, Dec. 2004.
- [3] A. J. Goldsmith and P. P. Varaiya, "Capacity of fading channels with channel side information," vol. 43, pp. 1986–1992, Nov. 1997.
- [4] M.-S. Alouini and A. J. Goldsmith, "Capacity of Rayleigh fading channels under different adaptive transmission and diversity-combining techniques," vol. 48, pp. 1165–1181, Jul. 1999.
- [5] A. J. Goldsmith and S.-G. Chua, "Variable-rate variable-power MQAM for fading channels," vol. 45, pp. 1218–1230, Oct. 1997.
- [6] M.-S. Alouini and A. J. Goldsmith, "Adaptive modulation over Nakagami fading channels," *Wireless Personal Comm.*, vol. 13, pp. 119–143, 2000.
- [7] M. O. Hasna, "On the capacity of cooperative diversity systems with adaptive modulation," in *Wireless and Optical Communications Networks, 2005. WOCN 2005. Second IFIP International Conference on*, Mar. 2005, pp. 432–436.
- [8] K. S. Hwang, Y. Ko, and M.-S. Alouini, "Performance analysis of opportunistic incremental relaying with adaptive modulation," in *Proc. IEEE International Symposium on Wireless Pervasive Computing 2008*, May 2008.
- [9] T. Nechiporenko, K. T. Phan, C. Tellambura, and H. H. Nguyen, "On the capacity of Rayleigh fading cooperative systems under adaptive transmission," *IEEE Trans. Wireless Commun.*, vol. 8, no. 4, pp. 1626–1631, Apr. 2009.
- [10] —, "Performance analysis of adaptive M-QAM for Rayleigh fading cooperative systems," in *Proc. IEEE International Conference on Communications (ICC)*, May 2008, pp. 3393–3399.
- [11] T. Nechiporenko, P. Kalansuriya, and C. Tellambura, "Performance of optimum switching adaptive M-QAM for amplify-and-forward relays," *IEEE Trans. Veh. Technol.*, vol. 58, no. 5, pp. 2258–2268, Jun. 2009.
- [12] P. Kalansuriya and C. Tellambura, "Performance analysis of decode-and-forward relay network under adaptive M-QAM," in *Proc. IEEE International Conference on Communications (ICC)*, 2009.
- [13] A. Sendonaris, E. Erkip, and B. Aazhang, "User cooperation diversity part II: implementation aspects and performance analysis," vol. 51, pp. 1939–1948, Nov. 2003.
- [14] D. Chen and J. N. Laneman, "Modulation and demodulation for cooperative diversity in wireless systems," *IEEE Trans. Wireless Commun.*, vol. 5, no. 7, pp. 1785–1794, Jul. 2006.
- [15] T. Wang, A. Cano, G. B. Giannakis, and J. N. Laneman, "High-performance cooperative demodulation with decode-and-forward relays," *IEEE Trans. Commun.*, vol. 55, no. 7, pp. 1427–1438, Jul. 2007.
- [16] Z. Yi and I.-M. Kim, "Decode-and-forward cooperative networks with relay selection," in *Vehicular Technology Conference, 2007. VTC-2007 Fall. IEEE 66th, Sep./Oct. 2007*, pp. 1167–1171.
- [17] B. Choi and L. Hanzo, "Optimum mode-switching-assisted constant-power single- and multicarrier adaptive modulation," vol. 52, no. 3, pp. 536–560, May 2003.
- [18] A. R. Leyman, X. Liu, H. K. Garg, and Y. Xin, "Automatic classification of imperfect QAM constellation using radon transform," in *Communications, 2007. ICC '07. IEEE International Conference on*, Glasgow, Jun. 2007, pp. 2635–2640.
- [19] L. De Vito, S. Rapuano, and M. Villanacci, "An improved method for the automatic digital modulation classification," in *Instrumentation and Measurement Technology Conference Proceedings, 2008. IMTC 2008. IEEE*, Victoria, BC, May 2008, pp. 1441–1446.
- [20] A. Doufexi, S. Armour, M. Butler, A. Nix, D. Bull, J. McGeehan, and P. Karlsson, "A comparison of the HIPERLAN/2 and IEEE 802.11a wireless LAN standards," *IEEE Commun. Mag.*, vol. 40, no. 5, pp. 172–180, May 2002.
- [21] W. Xiang, P. Richardson, and J. Guo, "Introduction and preliminary experimental results of wireless access for vehicular environments (WAVE) systems," in *Mobile and Ubiquitous Systems - Workshops, 2006. 3rd Annual International Conference on*, San Jose, CA, Jul. 2006, pp. 1–8.
- [22] T. Wang, A. Cano, and G. B. Giannakis, "Efficient Demodulation in Cooperative Schemes Using Decode-and-Forward Relays," in *Signals, Systems and Computers, 2005. Conference Record of the Thirty-Ninth Asilomar Conference on*, Oct./Nov. 2005, pp. 1051–1055.
- [23] N. C. Beaulieu and C. Cheng, "Efficient Nakagami-m Fading channel Simulation," *IEEE Trans. Veh. Technol.*, vol. 54, no. 2, pp. 413–424, Mar. 2005.
- [24] S. Ikki and M. H. Ahmed, "Performance analysis of cooperative diversity wireless networks over Nakagami-m fading channel," vol. 11, pp. 334–336, Jul. 2007.
- [25] I. Gradshteyn and I. Ryzhik, *Table of Integrals, Series, and Products, Sixth Edition*. Academic Press, 2000.